Pergamon

0301-9322(93)E0002-M

Int. J. Multiphase Flow Vol. 20, No. 1, pp. 99–116, 1994

0301-9322/94 $6.00 + 0.00

MULTI-DROPLET INTERACTION EFFECTS IN DENSE SPRAYS

I. SILVERMAN† and W. A. SIRIGNANO

Department of Mechanical and Aerospace Engineering, University of California, Irvine, CA 92717, U.S.A.

(Received 8 November 1992; in revised form 10 October 1993)

Abstract—A new approach for dense-spray modeling is employed to develop a model for multi-droplet interaction effects. A statistical description of droplets in a cloud and correlation functions for the effects of interactions between neighboring droplets are used to extract correction factors for various parameters that are affected by droplet interactions (e.g. drag coefficient, Nusselt number and Sherwood number). The correction factors enable the calculation of the drag coefficient, evaporation rate and heat transfer of a droplet in a cloud based on models for a single droplet. The model is employed to study the effects of droplet interactions on the evaporation and motion of a dense spray in a hot gaseous environment. It is shown that interaction effects are important during a larger fraction of the droplet lifetime as the droplet size decreases. The multi-droplet interactions cause the drag coefficient of a droplet in a dense spray to be lower—and hence its velocity higher—than that for an isolated droplet. For 100 μm droplets, as expected, the evaporation rate decreases and the droplet lifetime increases due to multi-droplet interactions. For 40 μm droplets, however, the evaporation rate increases and the droplet lifetime decreases. Although heat transfer to an interacting droplet is slower than to an isolated droplet, at the same gas-phase conditions and relative velocity of the droplets, the higher relative velocity of a 40 μm interacting droplet more than compensates for this effect to result in a shorter droplet lifetime.

Key Words: dense-spray, interactions, dispersion, statistical analysis modeling

1. INTRODUCTION

Typical dispersed two-phase flows encountered in engineering applications such as combustion systems and chemical processes have regions of large concentration of particles or droplets. In such regions, the effects of neighboring droplets modify the ambient conditions in the flow near any given droplet. Furthermore, the drag coefficient, Nusselt number and Sherwood number can be affected. Since the dimensions of a typical combustion chamber are of the order of 10–100 cm, while the droplets are of the order of $\leqslant 100\ \mu$m, computational resolution of the order of the drop size is impossible. In order to overcome the resolution problem, models for the effects of interactions between the droplets should be developed.

The need for interaction modeling has motivated a recent interest in the study of interactions between droplets. Most of the existing work on evaporating droplet interactions has primarily concentrated on droplets in artificial arrays and droplet streams. A detailed review of droplet array theory is provided by Sirignano (1983). Although array studies are useful to obtain a basic understanding of the effects of interactions on the heat and mass transfer to and from the droplets, their use is limited. Most combustion processes involve sprays, where only statistical information on the location of the droplet is available.

A more appropriate way to study droplet interactions is through the cloud or group approach, which utilizes statistical averaging. This approach was used by Labowsky & Rosner (1978), Correa (1981), Bellan & Cuffel (1983) and others. However, most of these studies neglect forced convection and thus are simply a diffusion analysis. Bellan & Harstad (1987, 1988) studied the evaporation of a droplet cloud in a convective flow but accounted only for non-hydrodynamic interactions (i.e. build-up of fuel vapor concentration in and cooling of the gas-phase environment).

†Present address: Propulsion Physics Division, Soreq Nuclear Research Center, Yavne 70600, Israel.

A new approach for cloud modeling is presented in this paper. Recent studies by Chiang & Sirignano (1993), Chiang *et al.* (1992), Kim *et al.* (1992, 1993) and others provide detailed information about interactions between droplets which travel in tandem or side-by-side in parallel. These studies involve the solution of Navier–Stokes, energy and species equations for a flow past 2 or 3 droplets. The results of these studies provide correlations for the interaction effects that account for the hydrodynamic as well as non-hydrodynamic interactions between the droplets.

A statistical description of droplets in a cloud, together with a model for its evolution in time and correlation functions for the effects of interactions between 2 neighboring droplets are used to extract correction factors due to multi-droplet interactions in dense sprays for various parameters (e.g. drag coefficient, Nusselt number and Sherwood number). The corrections factors are used to calculate the drag coefficient, lift coefficient, evaporation rate and heat transfer rate of a droplet in a cloud based on models for a single droplet. By employing correlation functions for the effects of interactions between two solid particles, this model can be used to account for multi-particle interactions in dense clouds of particles.

The next section describes the statistical description of the droplets in the cloud and the calculation of the correction factor. Section 3 addresses the evolution of the parameters of the statistical description of the cloud as it travels through the gas phase. Finally, in section 4, the model is used to obtain results for the evaporation and motion of a dense cloud of droplets in a hot ambient gas.

2. THE CORRECTION FACTOR FOR SINGLE-DROPLET LAWS DUE TO NEIGHBORING DROPLETS

The calculation of a correction factor for a droplet parameter due to multi-droplet interactions with neighboring droplets is based on correlation functions for the effects of an upstream droplet and a droplet that travels side-by-side in parallel to the droplet. However, in reality, the position of a neighboring droplet is neither exactly upstream nor directly perpendicular to the droplet direction of motion. Thus, two more correction functions that are based on the azmuthal position of the neighboring droplet relative to the droplet direction of motion are needed. See figure 1 for the geometry of a neighboring droplet. These functions correct the correlation functions which are based on the distance between the droplets for azimuthal positions that are different from those for which the correlation functions were calculated. In this work, assumptions regarding the forms and parameters of the correction functions will be made, since almost no experimental or theoretical data is available for them. One exception is the work of Rowe & Henwood (1961), who measured the drag coefficient of a sphere with a neighboring droplet located at different distances and relative azimuthal positions.

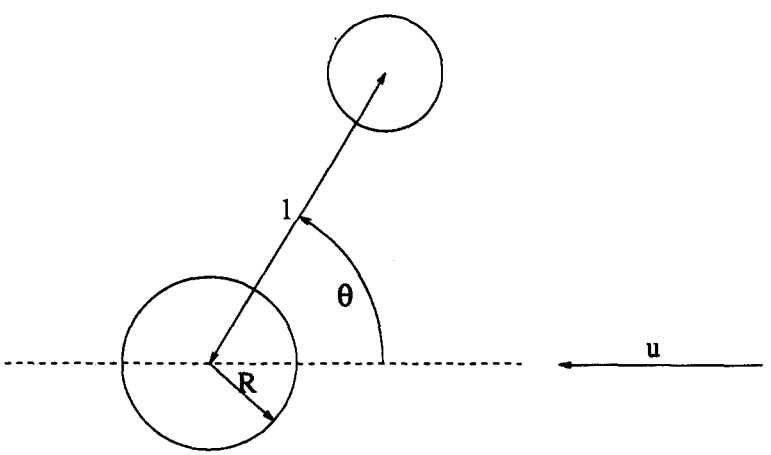

Figure 1. The geometry of a neighboring droplet.

Four functions are used to calculate the correction factor: $\Omega_u(l)$ and $\Omega_p(l)$ are correlation functions due to neighboring droplets that are located exactly upstream from or to the side of the droplet, respectively; and $\Phi_u(\theta)$ and $\Phi_p(\theta)$ are correction functions due to an azimuthal position that is not exactly upstream or aside. With these functions, the ratio of a general parameter Ψ for a droplet influenced by a neighboring droplet to the value of Ψ for an isolated droplet is constructed as

$$\frac{\Psi}{\Psi_{iso}} = [1 + \Omega_u(l)\Phi_u(\theta)][1 + \Omega_p(l)\Phi_p(\theta)], \quad [1]$$

where l and θ are the position coordinates of the neighboring droplet relative to the droplet and its direction of motion.

The position coordinates of the neighboring droplet, l and θ, are random variables whose probability distribution functions depend on the distribution of the droplets inside the cloud. The distribution function of the droplets within the cloud can be described by its mean value (μ_x, the average location of the droplets) and variance (σ_x). In order to extract the relation between the parameters of the distribution of the droplets within the cloud and the average distance between neighboring droplets, the following assumption is used. It is assumed that the average instantaneous distance between droplets in the actual cloud (l_{av}) is equal to the distance between droplets in a circular cloud, with the same number of droplets, in which the droplets are distributed uniformly. This cloud will be called the uniform cloud. The probability of finding, in the uniform cloud, a specific droplet within dr, $d\theta$ and $d\varphi$ of the point (r, θ, φ) (spherical coordinates) is given by

$$f_n(r, \theta, \varphi) = \frac{r^2 \sin(\theta)}{\frac{4}{3}\pi R_c^3} dr\, d\theta\, d\varphi \begin{cases} 0 \leqslant r \leqslant R_c \\ 0 \leqslant \theta \leqslant \pi \\ 0 \leqslant \varphi \leqslant 2\pi, \end{cases} \quad [2]$$

where r is distance from the center of the cloud and R_c is the radius of the cloud. The radius of the cloud, the number of droplets in it (N) and their number density (n) are related through the function

$$R_c = \left(\frac{3N}{4\pi n}\right)^{1/3}. \quad [3]$$

For the distribution function given in [2], the variance of the droplet distance from the center is

$$\sigma_r^2 = \frac{4\pi n R_c^5}{5N} = \frac{3}{5} R_c^2. \quad [4]$$

Demanding that both clouds have the same variance (i.e. $\sigma_r^2 = \sigma_x \cdot \sigma_x$) gives

$$n = \frac{3}{4\pi}\left(\frac{3}{5}\right)^{3/2} N|\sigma_x|^{-3}, \quad [5]$$

where σ_x is the variance of the droplet distribution function in the original cloud.

In the uniform cloud, the distance between any 2 neighboring droplets is l. Hence, if each droplet is surrounded by an imaginary sphere of radius $l/2$, these imaginary spheres touch each other and do not overlap. Knowing the number density of the droplets within the cloud, the volume of each sphere can be calculated from the following relation:

$$V = \frac{\epsilon}{n} \quad [6]$$

where ϵ is the volume fraction occupied by these imaginary spheres. If the droplets in the uniform cloud are arranged in a face-centered cubic (FCC) lattice arrangement, $\epsilon = 0.7405$. It is still questionable whether ϵ can be higher—see Conway & Sloane (1988). The best upper bound today for ϵ is 0.7784.

Employing [6], the distance between 2 neighboring droplets is given by the diameter of these spheres:

$$l = \left(\frac{6V}{\pi}\right)^{1/3} = 2.582\left(\frac{\epsilon}{N}\right)^{1/3}|\sigma_x|. \quad [7]$$

According to the previous assumption, this is the average instantaneous distance between neighboring droplets in the actual cloud.

The distribution function for the distance to a neighboring droplet in the actual cloud will be assumed to have a maximum at the average distance between neighboring droplets and go to zero as the distance goes to infinity. A reasonable choice is

$$f_1(l) = z \exp(-z), \quad 0 \leqslant z < \infty, \tag{8}$$

with

$$z = \frac{l - 2R}{l_{av} - 2R},$$

where l_{av} is the average distance between neighboring droplets.

The probability of finding a neighboring droplet in any azimuthal position around a given droplet is equal. If there are a few neighboring droplets, each one has equal probability inside a sector of the space around the droplet. In order to determine how many neighbors a droplet has, it is assumed again that the droplets are distributed uniformly and each is surrounded by an imaginary sphere of radius $l_{av}/2$. The spheres touch each other and do not overlap. It has been found that, at most, 12 spheres can be arranged so that they all touch a single sphere. See Conway & Sloane (1988, p. 21) for a review of this ancient geometrical question. One specific arrangement that complies with this requirement is the FCC lattice mentioned earlier. Hence, it is taken that each droplet inside the cloud has 12 neighboring droplets which are spaced evenly around it. Symmetrical considerations indicate that 6 neighboring droplets are in the upstream hemisphere. One is located almost directly upstream such that its θ coordinate is in the range $0 \leqslant \theta \leqslant 30$, while the other 5 are in the range $30 \leqslant \theta \leqslant 90$. For another 5, $90 \leqslant \theta \leqslant 150$ is the range and the last droplet is located downstream with $150 \leqslant \theta \leqslant 180$. Thus, a uniform distribution function is taken for the azimuthal position of a neighboring droplet:

$$f_2(\theta) = \frac{1}{\theta_1 - \theta_0}, \quad \theta_0 \leqslant \theta \leqslant \theta_1, \tag{9}$$

where the limits on the azimuthal position are different for each neighboring droplet (e.g. for the neighboring droplet which is located almost directly upstream $\theta_0 = 0$ and $\theta_1 = 30$).

Using the distribution functions of l and θ, the mean value of the correction due to interactions, [1], with a randomly located neighboring droplet is

$$\mu_\Psi = \int_{2R}^{\infty} \int_{\theta_0}^{\theta_1} [1 + \Omega_u(l)\Phi_u(\theta)][1 + \Omega_p(l)\Phi_p(\theta)]F(l, \theta)\, d\theta\, dl, \tag{10}$$

where $F(l, \theta) = f_1(l)f_2(\theta)$ since l and θ are independent random variables.

In order to calculate the correction factor due to the interactions of several neighboring droplets, an assumption is made that the effect of each droplet can be calculated separately. Since the coordinates of the neighboring droplets are independent random variables, the correction factor for single-droplet laws, due to multi-droplet interactions, is given by

$$\Delta_\Psi = \prod_{i=1}^{K} \mu_\Psi^{(i)}, \tag{11}$$

where K is the number of neighboring droplets that affect the droplet. Note that, Ω_u and Ω_p are the result of non-linear interactions between only 2 droplets. Therefore, this assumption about the pairwise additivity of hydrodynamic interactions cannot be rigorously defended. However, this assumption has been used previously by Glendinning & Russel (1982), who found that it gives correct results for dilute sprays and predicts the correct variation as the density increases. Neglect of the effect of screening due to intervening droplets, which becomes important for dense sprays, is corrected here by accounting for the effect of only the K nearest neighbors.

3. THE EVOLUTION OF THE DROPLETS' DISPERSION

In the previous section, the correction factor for single-droplet laws, due to interactions between neighboring droplets in a dense spray, has been calculated. The correction factor depends on the distribution function of the droplets within the cloud through the expression for the average instantaneous distance between neighboring droplets, [7]. This distribution function changes, as the cloud of droplets travels through the gas phase, due to the velocity differences between the droplets. The velocity differences between the droplets, which may have several causes (e.g. turbulent gas motion or atomizer instabilities), normally cause the cloud to expand as the cloud travels through the gaseous environment. This expansion causes a spray that is initially dense to become dilute as it moves forward, away from the atomizer.

The Lagrangian equation for the velocity vector of a droplet is

$$\frac{dU_L}{dt} = C_D \frac{3\rho}{8\rho_L R}(U - U_L)|U - U_L|, \tag{12}$$

where

$$C_D = \frac{24}{Re_d}\left(1 + \frac{Re_d^{2/3}}{6}\right)\Delta_{Cd}(Re_d, \dots), \tag{13}$$

$$Re_d = 2\frac{R}{\nu}|U - U_L| \tag{14}$$

and $\Delta_{Cd}(Re_d, \dots)$ is the correction factor for the drag coefficient due to multi-droplet interactions. In order to calculate the dispersion of the droplets, the velocity vector of the droplet is divided into two components:

$$U_L = \bar{U}_L + U'_L \tag{15}$$

where $\bar{U}_L$ is the average velocity vector of the droplets in the cloud and U'_L is a vector of the difference between the velocity vector of a particular droplet and the average velocity vector; $\bar{U}_L$ is a deterministic variable while U'_L is random. O'Rourke (1989) developed the turbulent dispersion model of Dukowicz (1980) to explore the statistical properties of U'_L due to the turbulent motion of the gas phase. Here, the same procedure is employed to study the effects of the initial differences in the velocities of the droplets, due to atomization, on their dispersion in a laminar flow field. It is assumed that the components of the initial velocity difference vector, U'_L, are random variables with the following distribution function:

$$f(U'_{L0,i}) = \frac{1}{\sqrt{2\pi}\sigma_{u0,i}} \exp\left[-\frac{(U'_{L0,i})^2}{2\sigma^2_{u0,i}}\right], \quad -\infty < U'_{L0,i} < \infty; \quad i = 1, 2, 3. \tag{16}$$

Substitution of [13]–[15] into [12] gives the following equations for the average velocity and the velocity differences:

$$\frac{d\bar{U}_L}{dt} = \frac{9\nu\rho}{2\rho_L R^2}\left(1 + \frac{\bar{Re}_d^{2/3}}{6}\right)\Delta_{Cd}(U - \bar{U}_L) \tag{17}$$

and

$$\frac{dU'_L}{dt} = \frac{9\nu\rho}{2\rho_L R^2}\left[\left(1 + \frac{Re_d^{2/3}}{6}\right)\Delta_{Cd}(U - \bar{U}_L - U'_L) - \left(1 + \frac{\bar{Re}_d^{2/3}}{6}\right)\Delta_{Cd}(U - \bar{U}_L)\right], \tag{18}$$

where

$$\bar{Re}_d = 2\frac{R}{\nu}|U - \bar{U}_L|. \tag{19}$$

Generally, [18] should be solved numerically. For one-dimensional flow, when the average relative velocity of the droplets is much larger than the velocity differences between the droplets (i.e. $|U - \bar{U}_L| \gg |U'_L|$) and after neglecting terms of order $O(U'_L \cdot U'_L)$, [18] becomes

$$\frac{du'_L}{dt} = -\frac{9\nu\rho}{2\rho_L R^2} u'_L \left[\left(1 + \frac{\overline{Re}_d^{2/3}}{6}\right) \Delta_{Cd} + \overline{Re}_d \left(\frac{1}{9} \overline{Re}_d^{-1/3} \Delta_{Cd} + \left(1 + \frac{\overline{Re}_d^{2/3}}{6}\right) \frac{d(\Delta_{Cd})}{d\, Re_d} \bigg|_{Re_d = \bar{Re}_d} \right) \right], \quad [20]$$

where u, $\bar{u}_L$ and u'_L are the non-zero components of U, $\bar{U}_L$ and U'_L, respectively. The solution of [20] is

$$\frac{u'_L}{u'_{L0}} = \exp\left(-\int_0^t \frac{9\nu\rho}{2\rho_L R^2} \left[\left(1 + \frac{\overline{Re}_d^{2/3}}{6}\right) \Delta_{Cd} + \overline{Re}_d \left(\frac{1}{9} \overline{Re}_d^{-1/3} \Delta_{Cd} + \left(1 + \frac{\overline{Re}_d^{2/3}}{6}\right) \frac{d(\Delta_{Cd})}{d\, Re_d} \bigg|_{Re_d = \bar{Re}_d} \right) \right] d\tau \right). \quad [21]$$

This solution shows that the velocity differences decay exponentially in time. Even if U'_L is calculated numerically by [18], as necessary under most conditions, the ratio of the instantaneous velocity differences to the initial velocity differences is still a deterministic function of time (for a laminar flow field):

$$\frac{U'_{L,i}}{U'_{L0,i}} = A_i(t), \quad i = 1, 2, 3. \quad [22]$$

For turbulent flows, the functions $A_i(t)$ are non-deterministic, due to the stochastic nature of U. The reader is referred to O'Rourke (1989) for details on how to calculate $A_i(t)$ in a case of a turbulent flow.

While [17] can be used to calculate the trajectory of the center of the cloud, the equation for the velocity differences is employed to calculate the expansion of the cloud. The center of the cloud at $t = 0$ was prescribed to be the initial average location of the droplets. If the velocity differences of the droplets are known, the position displacement of a droplet, relative to the location of the center of the cloud, is given by

$$X' = X'_0 + \int_0^t U'_L(\tau)\, d\tau, \quad [23]$$

where X'_0 is the initial relative position vector of the droplet. There may be some correlation between the initial distribution functions for the velocity differences and the relative position of the droplets. However, there is no need to define their joint distribution function. It is sufficient to assume that [16] is the marginal distribution function with respect to U'_L (i.e. the distribution function obtained after integration of the joint distribution function over the range of X'). Using [23] and [22], the mean positions of the droplets in each direction (mean of X') are

$$\mu_{x,i} = \mu_{x0,i} + \mu_{u0,i} \int_0^t A_i(\tau)\, d\tau = 0, \quad i = 1, 2, 3, \quad [24]$$

since, from [16], the average initial velocity difference is zero. Hence, the center of the cloud coincides with the instantaneous average position of the droplets. The variances of the components of the vector X' are given by

$$\sigma^2_{x,i} = \sigma^2_{x0,i} + 2E(X'_{0,i}, U'_{L0,i}) \int_0^t A_i(\tau)\, d\tau + \sigma^2_{u0,i} \left(\int_0^t A_i(\tau)\, d\tau \right)^2, \quad i = 1, 2, 3, \quad [25]$$

where

$$E(X'_{0,i} U'_{L0,i}) = \int_{-\infty}^{\infty} \int_{-\infty}^{\infty} X'_{0,i} U'_{L0,i} f(X'_{0,i}, U'_{L0,i})\, dX'_{0,i}\, dU'_{L0,i}, \quad i = 1, 2, 3. \quad [26]$$

If U'_{L0} and X'_0 are independent random variables then

$$\sigma^2_{x,i} = \sigma^2_{x0,i} + \sigma^2_{u0,i} \left(\int_0^t A_i(\tau)\, d\tau \right)^2, \quad i = 1, 2, 3. \quad [27]$$

The temporal variation of the variance of the droplets' distribution within the cloud, σ_x, provides all the necessary information regarding the expansion of the cloud because of the velocity differences between the droplets. As has been shown in section 2, this is all that is needed to calculate how the effects of interactions between neighboring droplets change as the cloud of droplets travels through the gas phase.

With [25] for the temporal variation of the distribution function variance, the dispersion velocity (the velocity at which the average distance between droplets increases) is given by differentiating [7] with respect to time:

$$\frac{dl}{dt} = 2.582\left(\frac{\epsilon}{N}\right)^{1/3}\frac{\dot{\sigma}_x \cdot \dot{\sigma}_x}{2|\sigma_x|} \qquad [28]$$

where the components of the $\dot{\sigma}_x$ vector are given by

$$(\dot{\sigma}_{x,i})^2 = 2E(X'_{0,i}U'_{L0,i})A_i(t) + 2\sigma^2_{u0,i}A_i(t)\int_0^t A_i(\tau)\,d\tau, \quad i = 1, 2, 3. \qquad [29]$$

Writing [28] as a function of the cloud mass and the size of the droplets gives

$$\frac{dl}{dt} = 2.582\left(\frac{4\pi\rho_L\epsilon}{3M}\right)^{1/3} R\frac{\dot{\sigma}_x \cdot \dot{\sigma}_x}{2|\sigma_x|}. \qquad [30]$$

For clouds with the same mass, velocity differences variance and position variance, [30] indicates that the dispersion velocity is larger for clouds with larger droplets. This occurs because the ratio of the droplet spacing to the droplet radius R, for fixed liquid mass, depends upon the cloud volume but is independent of the droplet radius. This effect can be seen in figure 7(a) for the case of a linear correlation between the droplet position and velocity differences. At $t = 0$ all clouds have the same

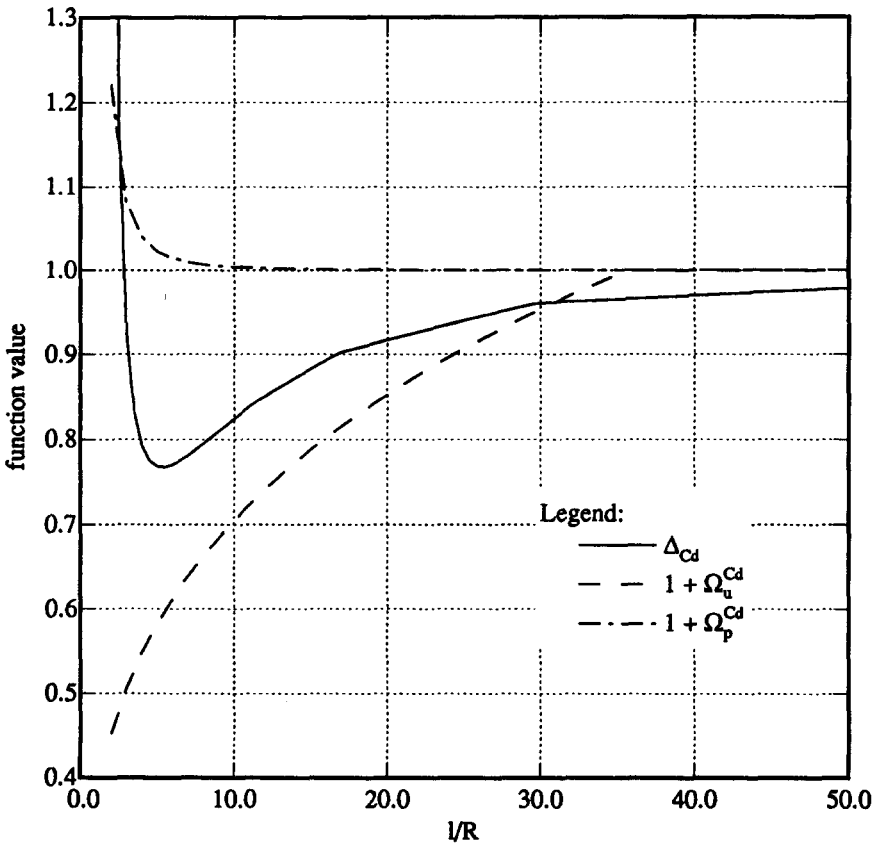

Figure 2. Drag coefficient correction factor and correlation functions for interaction effects due to an upstream or side droplet.

mass, velocity differences variance and position variance. As expected from [30], the dispersion velocity at $t = 0$ (the slope of the l vs t curves) is largest for the cloud of 100 μm droplets and smallest for the cloud of 40 μm droplets. In the other case presented in figure 7(a), the initial velocity differences and the initial position of the droplets are independent random variables. Hence, the dispersion velocity at $t = 0$ is identically zero and this effect cannot be noticed.

4. RESULTS AND DISCUSSION

We study the properties of the correction factor before examining the effects of multi-droplet interactions on the behavior of a dense spray. The correlation functions listed below were used in the computations. Note that the model does not put any limitations on the form and parameters of the correlation functions. Moreover, up to this point, the analysis is applicable to sprays as well as to clouds of solid particles.

Regarding the correction functions Φ_u and Φ_p, it is assumed that they are general and apply for any parameter Ψ that may be affected by droplet or particle interactions, Φ_u, the correction of Ω_u for θ different from zero, is taken to be

$$\Phi_u = \exp\left(\frac{-\theta^2}{\theta_w^2}\right), \quad \theta < 90, \qquad [31]$$

where θ_w is half of the upstream droplet wake angle, Φ_p, the correction of Ω_p for θ different from 90°, is taken to be

$$\Phi_p = \sin(\theta). \qquad [32]$$

The correlation functions Ω_u and Ω_p are different for droplets and particles and for each parameter Ψ. The functions Ω_u^{Cd} and Ω_p^{Cd} for the effects of interactions on the drag coefficient of

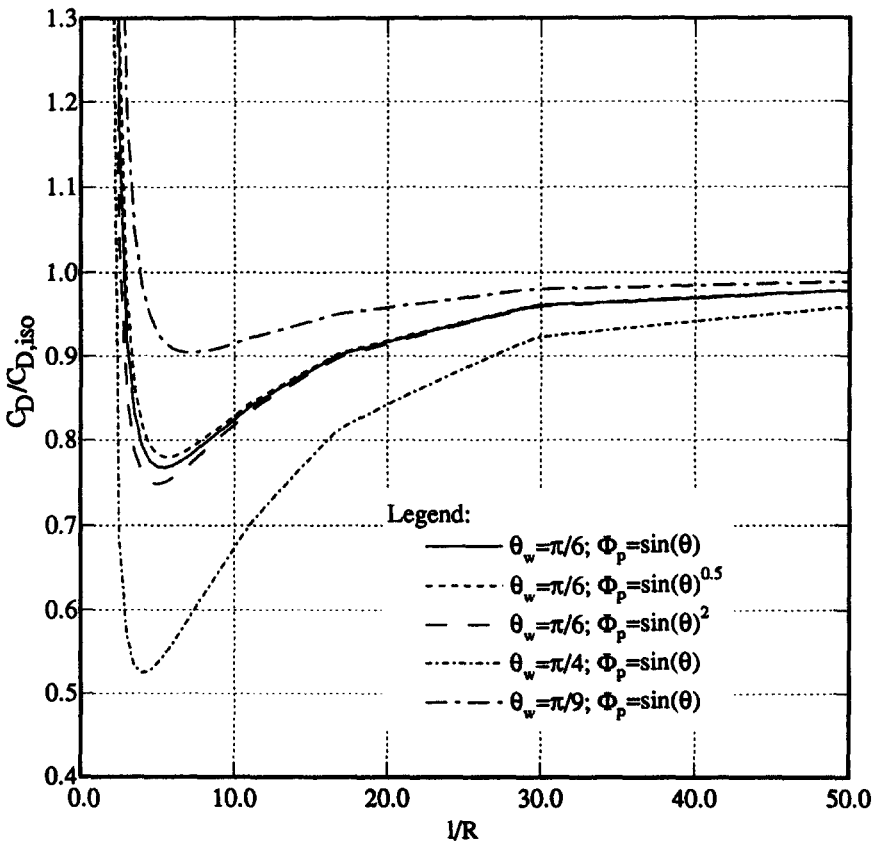

Figure 3. The effect of the azimuthal correction functions on the drag coefficient correction factor.

a droplet are taken from Chiang & Sirignano (1993) and Kim *et al.* (1993), respectively. Thus, from Chiang & Sirignano (1993), it is found that

$$[1 + \Omega_u^{Cd}(l)\Phi_u(0)] = 0.549\mathrm{Re}_m^{-0.098}(1 + B_{H,film})^{0.132}\left(\frac{l}{R_1}\right)^{0.275}\left(\frac{R_2}{R_1}\right)^{0.521}, \quad [33]$$

where $\Phi_u(0) = 1$. In this and the following correlations, Re_m is the droplet Reynolds number, $B_{H,film}$ is the heat transfer number and Pr_{film} is the Prandtl number [all calculated according to the average conditions in the boundary layer (film) around the droplet]. The index "1" denotes the upstream droplet and "2" is used for the downstream droplet. This correlation and the correlation given by [35] have been fitted to numerical results where $11 \leqslant \mathrm{Re}_m \leqslant 254$, $0.68 \leqslant \mathrm{Pr}_{film} \leqslant 0.91$, $0 \leqslant B_{H,film} \leqslant 2.52$ and $0.17 \leqslant R_2/R_1 \leqslant 2$. Based on data (in a case without heat or mass transfer) from Kim *et al.* (1993), the following correlation can be constructed:

$$\Omega_p^{Cd} = 0.62815\mathrm{Re}_m^{0.17287}\left(\frac{l}{R}\right)^{-2.4862}, \quad [34]$$

where here $50 \leqslant \mathrm{Re}_m \leqslant 150$ and the other parameters are constants—$\mathrm{Pr}_{film} = 1$, $B_{H,film} = 0$ and $R_2/R_1 = 1$.

As for the effect of droplet interactions on the heat transfer rate, Chiang & Sirignano (1993) found that the ratio of the Nusselt number (Nu) of an interacting droplet to the Nu of an isolated droplet can be approximated by

$$[1 + \Omega_u^{Nu}(l)\Phi_u(0)] = 0.528\mathrm{Re}_m^{-0.146}\mathrm{Pr}_{film}^{-0.768}(1 + B_{H,film})^{0.356}\left(\frac{l}{R_1}\right)^{0.262}\left(\frac{R_2}{R_1}\right)^{0.147}, \quad [35]$$

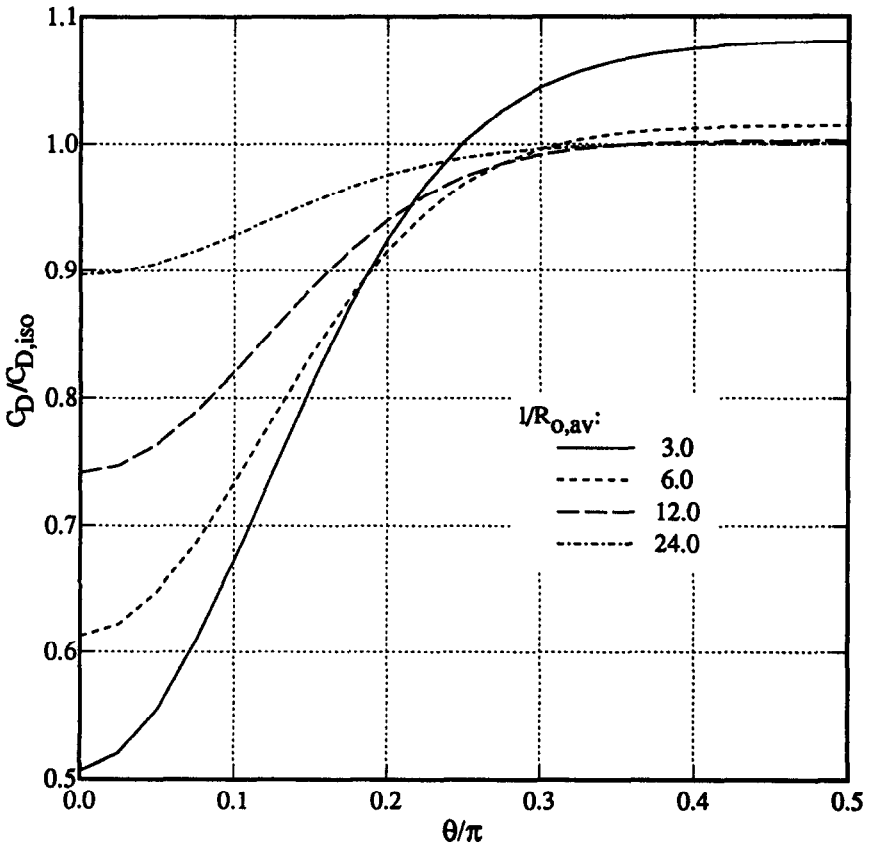

Figure 4. The combined correlation function for the drag coefficient vs the azimuthal position of a neighboring droplet.

while, based on heat transfer (without mass transfer) data from Tal & Sirignano (1981),

$$\Omega_p^{Nu}(l) = 1.250\left(\frac{l}{R}\right)^{-2.580} \quad [36]$$

where here $40 \leqslant Re_m \leqslant 150$, $0.5 \leqslant Pr_{film} \leqslant 5$ and $R_2/R_1 = 1$. The range for $B_{H,film}$ is not reported.

The dependence of the correlation factor, [10], for the drag coefficient on the average distance between neighboring droplets is shown in figure 2. It is calculated for a mono-size cloud, with $Re_d = 50$ and without heat transfer. The corresponding correlation functions, [33] and [34], are shown in figure 2. Generally, the correction factor decreases from unity as the average distance decreases. However, at very small distances ($l_{av} < 5R$), the effects of the neighboring side-by-side droplets cause an increase in the correction factor. As can be seen, the correction factor can become larger than unity if the droplets are very close (i.e. the drag coefficient of a highly interacting droplet is higher than that of an isolated droplet). The correlation functions for interaction between two neighboring droplets are equal to unity if the relative distance between the droplets is larger than 35. The correction factor, however, is lower than unity, even if the average distance between the neighboring droplets is larger than 35 since there might be some droplets at shorter distances for which interactions are significant. The effect of the assumed azimuthal correction functions on the results for the correction factor can be evaluated from figure 3. Figure 3 compares results for correction factors calculated with three wake angles for the Φ_u function and three different Φ_p functions. As can be seen in figure 3, the choice of the Φ_p function has little effect on the correction factor but the choice of the wake angle strongly affects its magnitude.

Figure 4 shows the dependence of the combined correlation function, given by [1], on the azimuthal position of the neighboring droplet. The qualitative behavior is similar to that presented

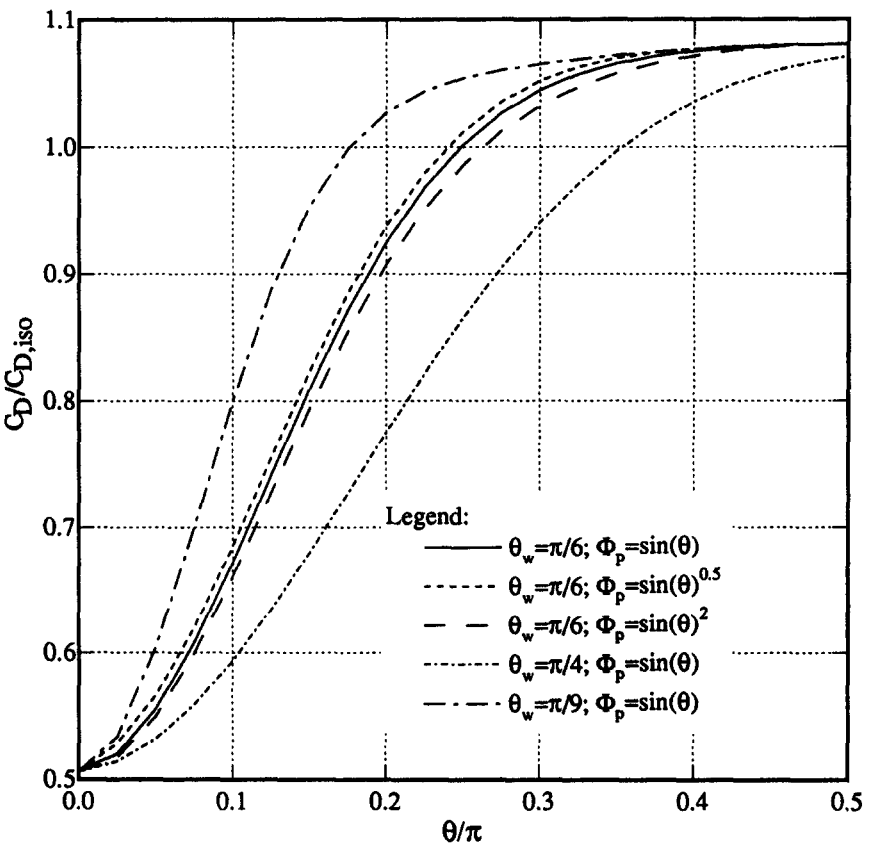

Figure 5. The effect of the azimuthal correction functions on the azimuthal variation of the combined correlation function for the drag coefficient, at $l = 3$.

by Rowe & Henwood (1961). Figure 5 shows the effect of changing the azimuthal correction functions on the results presented in figure 4 for $l = 3$. Again, the effect of changing the Φ_p function is very small, while the choice of the wake angle has a large effect. From the results presented by Rowe & Henwood (1961), it is clear that a constant value for the wake angle is physically incorrect if the distance to the neighboring droplet is less than 3. However, taking $\theta_w = \pi/6$ gives a good approximation for the azimuthal variation of the combined correlation function if $l > 3$.

In figure 6, we present results for the correction factor calculated for 6, 12 and 18 neighboring droplets. For the 6 neighbors case, 1 neighboring droplet is located ahead in the upstream direction, 4 on the sides and 1 behind. The location of the neighboring droplets for the 12 neighbors case has been described previously. For the case where each droplet has 18 neighbors, 1 neighboring droplet is located ahead in the upstream direction, 4 about 45° from the upstream direction, 8 on the sides, 4 more with an average $\theta = 135°$ and 1 downstream. As can be seen, the results are quite similar for all cases.

Finally, the last free parameter of the model is the volume fraction occupied by the imaginary spheres surrounding the droplets (ϵ). This parameter relates the droplets' distribution function to the average distance between neighboring droplets, [7]. Since it is a constant, a change in ϵ is equivalent to a change in the initial average distance between neighboring droplets. We assumed that $\epsilon = 0.7405$. It may be smaller if the droplets are packed in a less-dense arrangement. For example, if the droplets are located at the nodes of a three-dimensional rectangular grid $\epsilon = 0.5236$. However, since the third root of ϵ appears in [7], it represents a change of 11% in the initial average distance between neighboring droplets. As can be seen in figure 9, such a difference in the initial average distance has a negligible effect on a droplet history.

Figures 7–11 show the results for the evaporation and motion of dense clouds of droplets in a one-dimensional flow field. The initial droplet size for each cloud is different, but the mass and

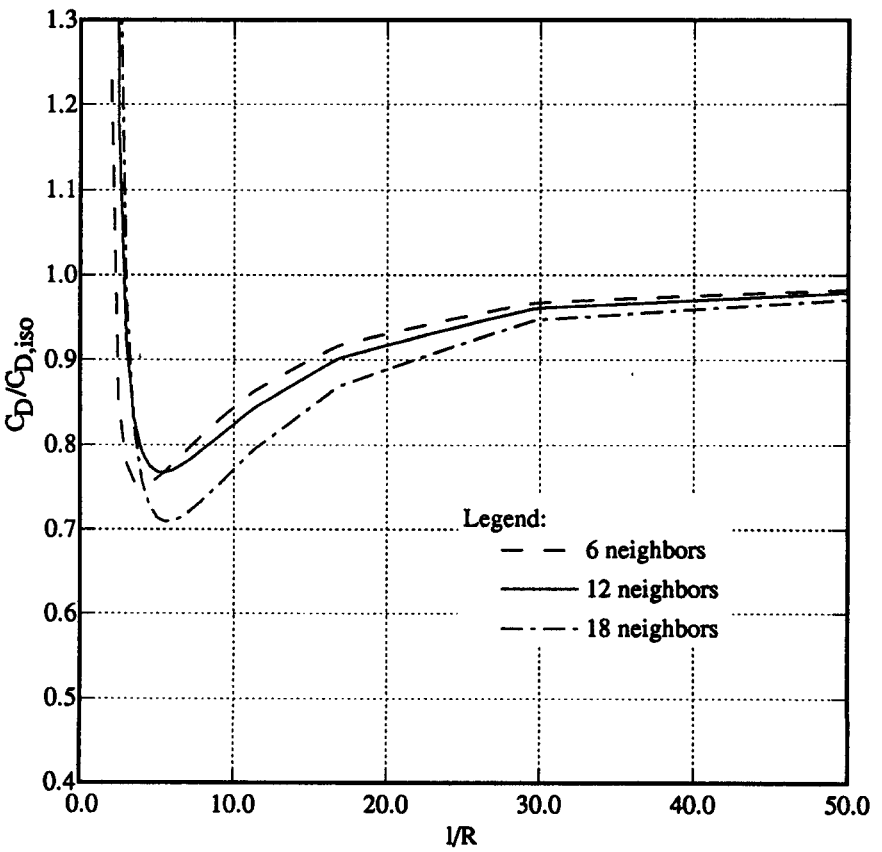

Figure 6. The effect of the number of neighboring droplets on the drag coefficient correction factor.

Table 1. The physical parameters used in the calculations

Gas phase	
Composition	Air
Velocity	1.0 [m/s]
Density	1.23 [kg/m^3]
Temperature	1200.0 [K]
Droplets	
Composition	n-Decane
Average velocity	20.0 [m/s]
Variance of the velocity differences	0.31 [m/s]
Velocity–location correlation	0
Initial average droplet radius	70.0 [μm]
Wake angle	$\pi/6$

Table 2. The initial parameters of the clouds

	Cloud No.		
	I	II	III
Initial radius of a droplet [μm]	40	60	100
Initial average distance between neighboring droplets [μm]	120	180	300
No. of droplets	536	159	34

radius of the clouds are kept constant. Hence, the number of droplets that form a cloud increases and the average distance between neighboring droplets decreases as the initial size decreases. The initial droplet sizes that were used for the calculations are 40, 60 and 100 μm. The model for the evaporation of a droplet is taken from Abramson & Sirignano (1989). The relevant data is given in tables 1 and 2. During parts of the simulations, the values of $\mathrm{Pr}_{\mathrm{film}}$ and $B_{\mathrm{H,film}}$ are out of the ranges for which the correlation functions have been constructed. Extrapolation of the correlation functions for these values gives erroneous results. Hence, if the actual value of a parameter is out of the range for which the correlation function has been constructed, the correlation function is calculated with the corresponding value of the parameter at the range limit (i.e. if the heat transfer number $B_{\mathrm{H,film}}$, becomes larger than 2.52, the correlations are calculated for $B_{\mathrm{H,film}} = 2.52$).

The calculations presented here were done with the assumption that the initial velocity differences and relative positions of the droplets are independent random variables. This assumption will now

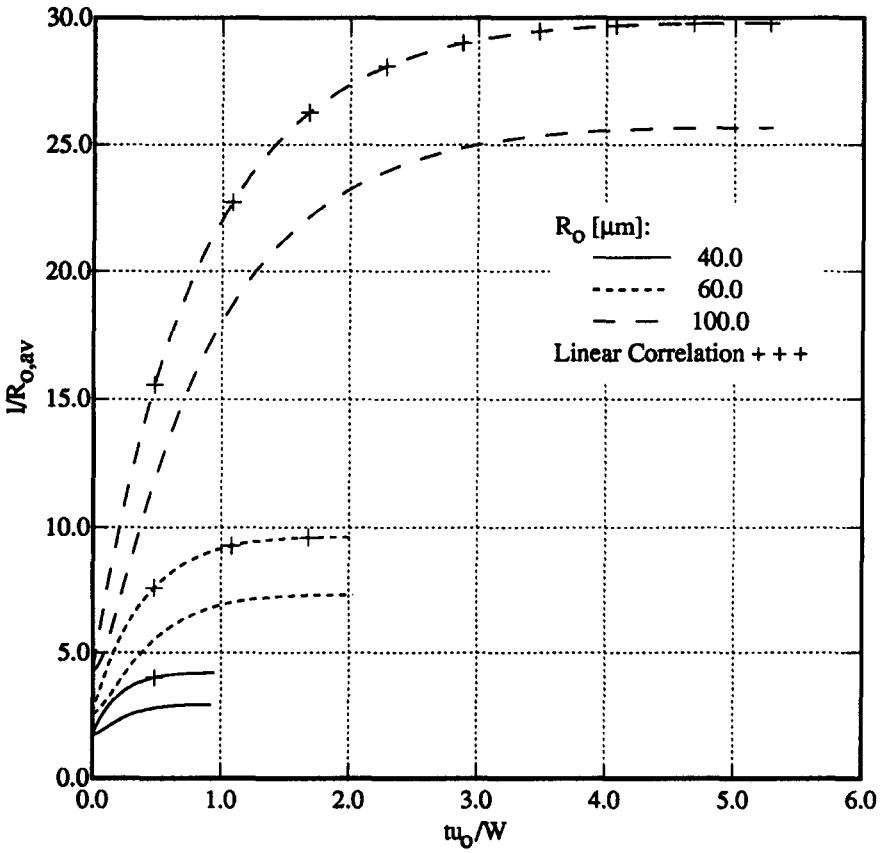

Figure 7(a). Time variation of the absolute distance between neighboring droplets.

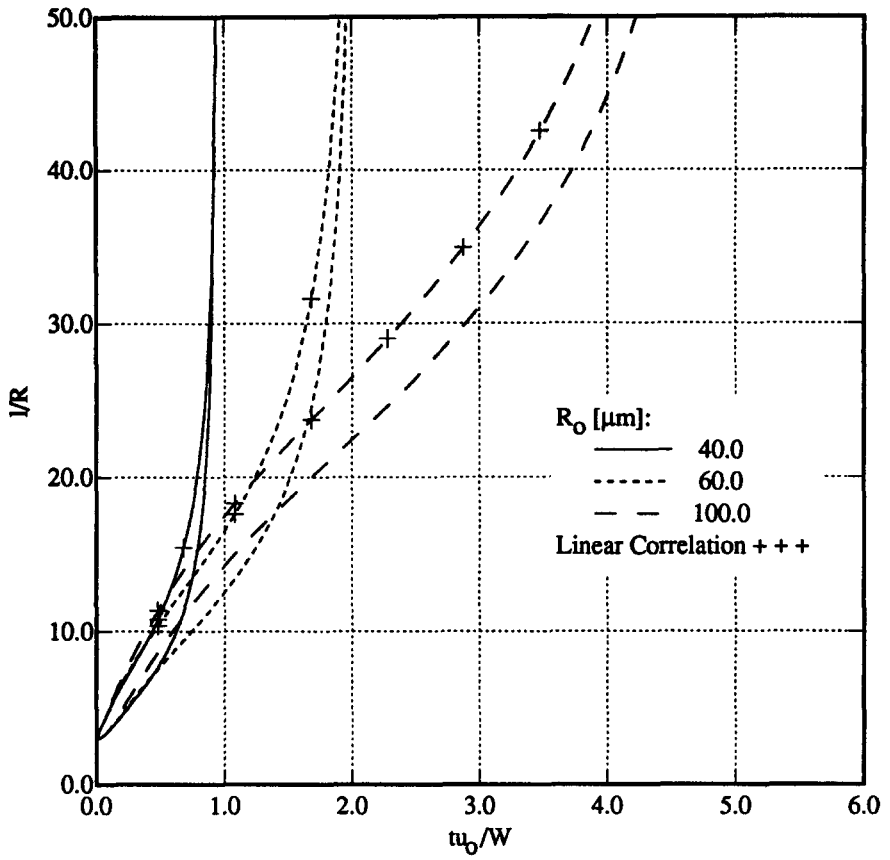

Figure 7(b). Time variation of the normalized distance between neighboring droplets.

be justified. Figure 7(a) presents the non-dimensional average distance between neighboring droplets and compares the results of two cases: (1) U'_{L0} and X'_0 are independent random variables; (2) there is a positive linear correlation between U'_{L0} and X'_0 (higher initial velocity difference corresponds to a higher initial displacement). As can be seen at $t = 0$, for the case where U'_{L0} and X'_0 are independent random variables, the initial dispersion velocity of the cloud is zero. If the initial velocity and initial position are independent random variables, there is an equal probability of finding, on the boundary of the cloud, a droplet that moves into or outside the cloud. Hence, the initial dispersion velocity is zero. As the droplets move, because of the velocity differences relative to the center of the cloud, a correlation between the droplet velocity difference and its position develops (i.e. droplets with high velocity differences move to the boundaries of the cloud and those with low velocity differences stay in the inner part of the cloud) and the dispersion velocity increases. For the other case, this correlation is already fully developed at $t = 0$ and the dispersion velocity is maximal at this time. If the correlation coefficient between the initial velocity and the position of a droplet were negative, the initial dispersion velocity is negative. This causes the number density to increase initially, but as the positive correlation develops the cloud starts to expand and the number density decreases. As can be seen in figure 7(a), the characteristic time for the development of the dispersion velocity is much shorter than the droplet lifetime. Although there is a moderate difference between the results for the average distance between the droplets for these two cases, no effect on the velocity or evaporation rate of the droplets has been noticed.

Regarding the results of the case where U'_{L0} and X'_0 are independent random variables, the average distance between neighboring droplets in the cloud of small droplets ($R_0 = 40\ \mu$m) does not change much throughout the droplet lifetime. However, the distance between the large droplets ($R_0 = 100\ \mu$m) increases by a factor of 5. There are two reasons for the smaller dispersion of a cloud into small droplets: the drag force causes greater acceleration of the small droplets so that their

velocity differences decay faster; therefore, with a larger number of small droplets, the dispersion velocity will be smaller.

The absolute distance between the droplets, however, is not the correct variable to study regarding the effects of droplet interactions. The interactions also depend on the size of the droplets, and the correct variable to study is the normal distance between the droplets. The normalized distance between the droplets is given by the ratio of the absolute distance to the instantaneous radius of the droplets. Figure 7(b) presents the normalized distance between the droplets. The absolute average distance between the small droplets remains almost constant in time but as they evaporate the normalized distance increases. For the large droplets, the initial evaporation rate is slow and their radius does not change much. However, their velocity differences decay slowly. Hence, the normalized distance between the large droplets changes mainly because of their dispersion. The relative importance of interaction on droplets of different initial sizes can be found from the data in figure 7(b). The normalized distance between 40 μm droplets reaches a value of 30 after 97.8% of their lifetime. 100 μm droplets reach this stage after only 54.7% of their lifetime.

Figure 8 compares results with and without accounting for droplet interactions. It displays the time variation of the velocity of the droplets and their radii. As expected, at the first stage of a droplet lifetime, when accounting for droplet interactions, the velocity of the droplets is higher since interactions lower the drag coefficient. However, while the evaporation rate of a 100 μm droplet decreases due to interactions, the evaporation rate of a 40 μm droplet increases and its lifetime is shorter. Although the heat transfer to a 40 μm interacting droplet is slower than to an isolated droplet of the same size (when the gas-phase conditions and the relative velocity of the droplets are the same), the higher relative velocity of a 40 μm interacting droplet more than compensates for this effect to result in a shorter droplet lifetime. The effect of the initial distance between neighboring droplets is displayed in figure 9. It appears not to have a major effect.

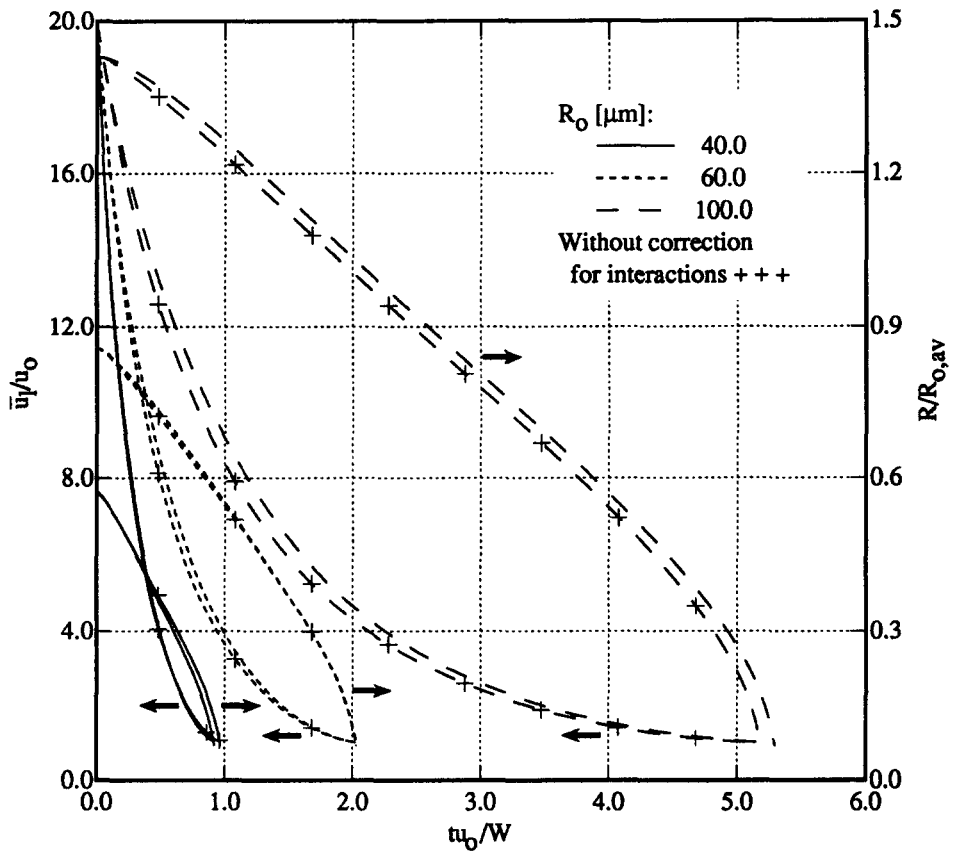

Figure 8. Time variation of the droplets' velocity and radius.

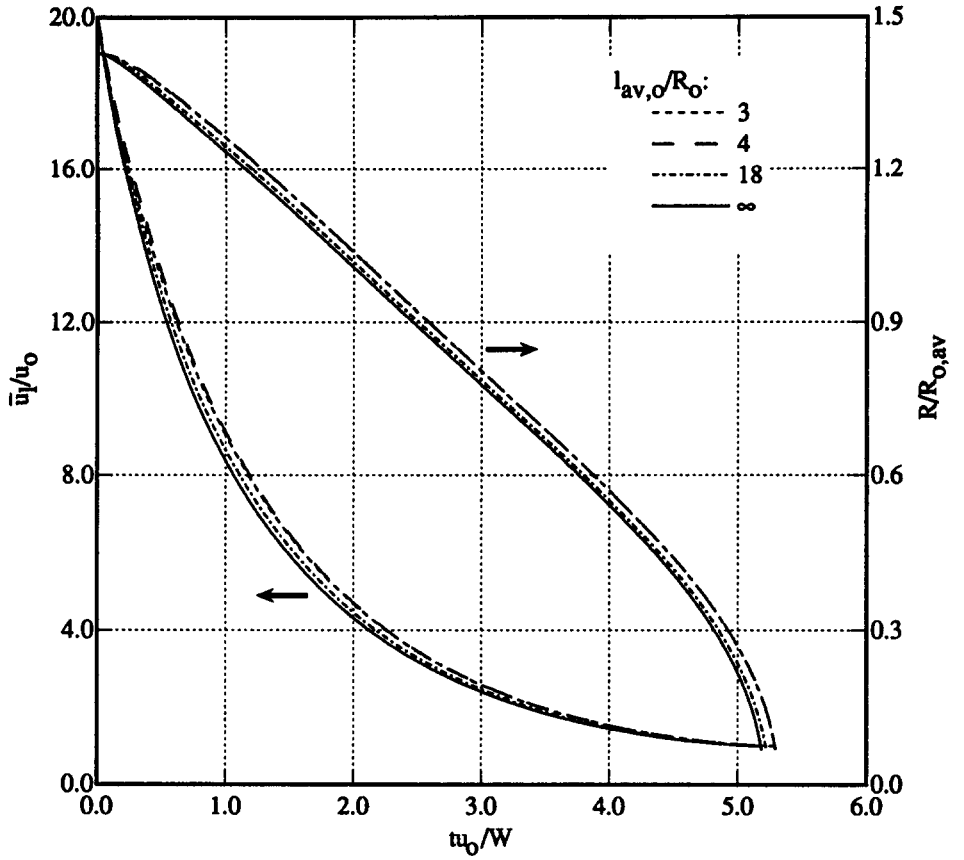

Figure 9. The effect of the initial average distance between neighboring droplets on the temporal variation of the velocity and radius of a droplet. Calculated for clouds without velocity differences between the droplets and an initial droplet radius of 80 μm.

Finally, the small total effect of interactions with a larger effect earlier in the droplet lifetime is shown by figures 10 and 11. Figure 10 shows the competing effects of correcting C_D and Nu for multi-droplet interactions. It displays the instantaneous evaporation rate of a 100 μm droplet ($\dot{m}$). Curve 1 have been calculated by accounting for the effects of interactions on both the drag coefficient and Nu, while curve 2 was calculated without accounting for interaction effects. When only the C_D is corrected for interaction effects, curve 3 is obtained. The higher droplets velocity, due to their lower corrected drag coefficient, causes the evaporation rate to increase. However, when only Nu is corrected for interaction effects (curve 4) the evaporation rate is lower initially, since the lower heat transfer rate causes the surface temperature to rise slower than for an isolated droplet. For a 100 μm droplet, the correction to Nu is more important than the correction to C_D and the total effect of interaction is to increase the droplet lifetime.

Figure 11 presents again the dependence of the drag coefficient correction factor on the average distance between neighboring droplets. Here however, the Re and heat transfer values used for the calculations were taken from the results for the evaporation and motion of a dense spray of 100 μm droplets in a one-dimensional flow field. The different curves are calculated with the actual conditions of the droplets at different times. For the conditions prevailing during most of the droplet lifetime, the correction factor is quite close to unity, except for early times and small spacings.

5. CONCLUSIONS

A new approach for dense-spray modeling is used in this paper to develop a model for multi-droplet interaction effects. This model is employed to calculate the effect of multi-droplet interactions on the evaporation and motion of a dense spray in a hot gaseous environment.

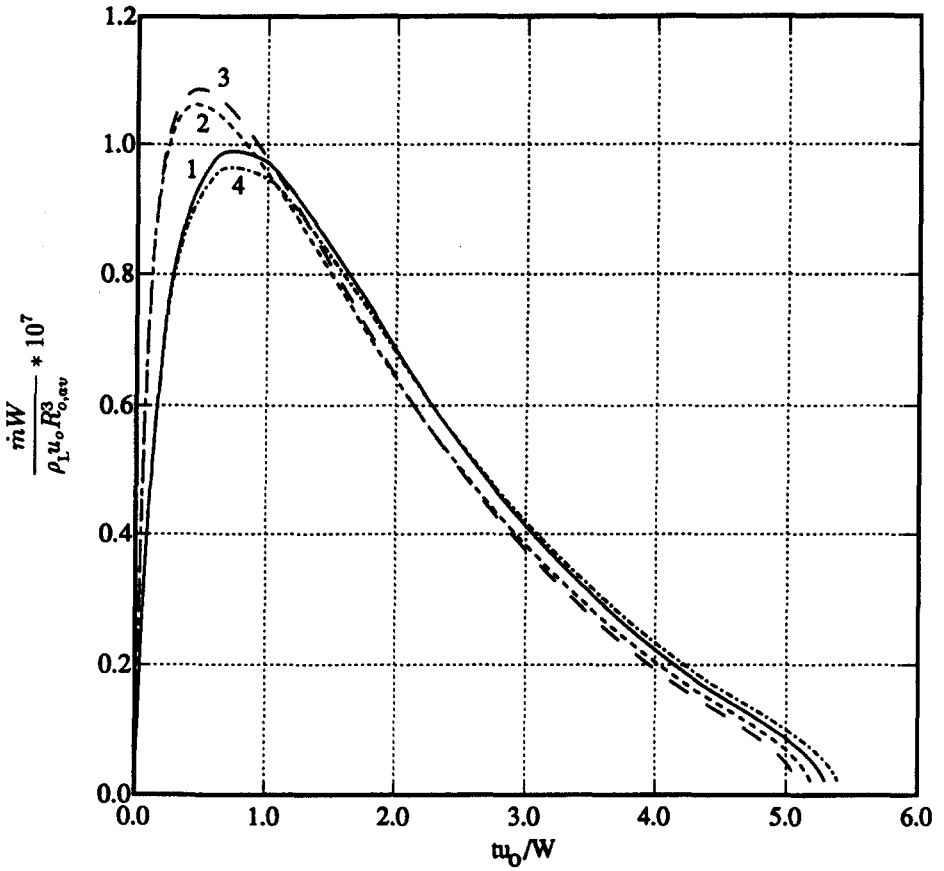

Figure 10. Instantaneous evaporation rate of a 100 μm droplet: (1) with interaction effects; (2) without interaction effects; (3) when only C_D is corrected for interaction effects; and (4) when only Nu is corrected for interaction effects.

It has been found that the dispersion velocity (i.e. the velocity at which the average distance between the droplets increases) of fine sprays is lower than for sprays of large droplets. The average correction factor due to multi-droplet interactions effects increases as the initial droplet size decreases (i.e. interactions affect small droplets more strongly than large droplets). The decay of the effects of interactions between small droplets is mainly due to the evaporation of the droplets. For large droplets, interaction effects decay mainly because of the dispersion of the droplets.

Multi-droplet interactions do not cause a monotonic change in the parameters that are affected by them (e.g. drag coefficient, Nu and Sherwood number) as the average distance between the droplets increases. The drag coefficient and Nu correction factors decrease as the average distance between the droplets increases for $l_{av} < 5R$ and increase as l_{av} increases for $l_{av} > 5R$.

The effect of multi-droplet interactions on the total behavior of the spray can be different than what is expected based on their effect on each parameter alone. The velocity of an interacting droplet is higher, for most of its lifetime, than for an isolated droplet because of the lower than unity correction factor for the drag coefficient. The effects of interactions on the heat transfer rate depend on the droplet size. For a large interacting droplet, the heat transfer rate is lower than for an isolated droplet. However, for a small droplet it is higher, although interactions cause a reduction of Nu at fixed Re. The higher relative velocity of the small droplets compensates by means of the Re and actually causes an increase in Nu.

More research on interactions between 2 droplets is needed in order to increase the accuracy of this model. The correlations for interaction effects due to 2 droplets which move side-by-side in parallel should be improved. Correlations for the effects of interactions on the drag coefficient, Nu and Sherwood number should be derived based on data from studies of moving droplets which

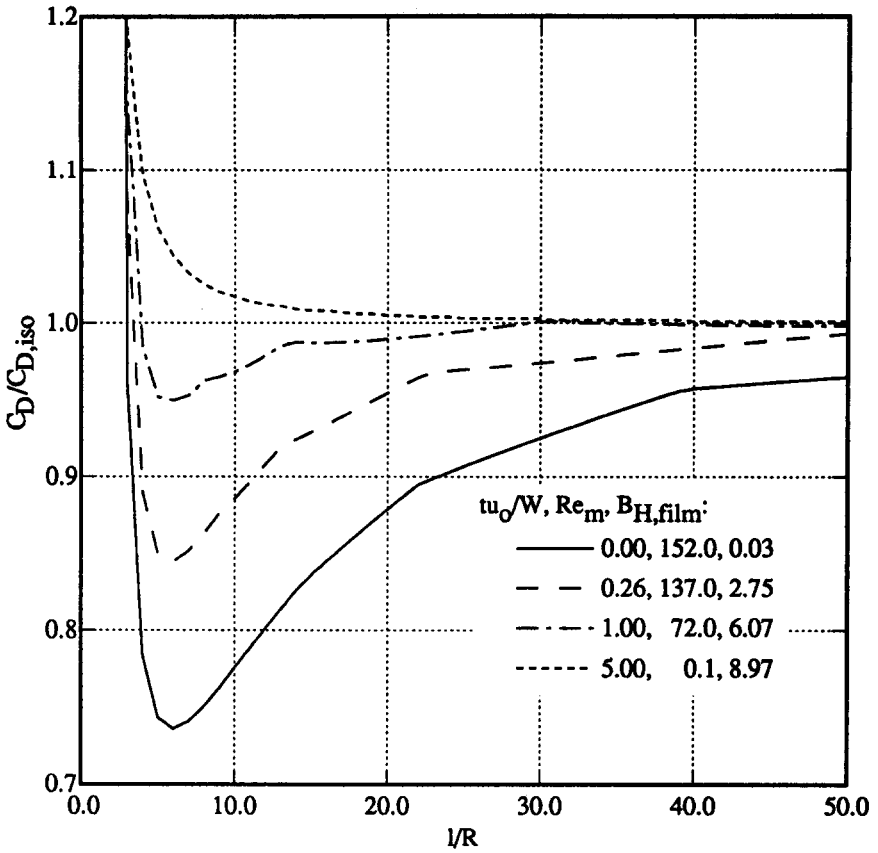

Figure 11. Drag coefficient correction factor for a 100 μm droplet. Re and heat transfer values are taken from the results for the evaporation and motion of a dense spray in a one-dimensional flow field.

include heat and mass transfer. The range of the correlation functions for 2 droplets in tandem should be expanded to the lower Re and higher heat and mass transfer numbers, which are encountered during the later stages of the droplet lifetime.

REFERENCES

ABRAMSON, B. & SIRIGNANO, W. A. 1989 Droplet vaporization model for spray combustion calculations. *Int. J. Heat Mass Transfer* **32,** 1605–1618.

BELLAN, J. & CUFFEL, R. 1983 A theory of non-dilute spray evaporation based upon multiple drop interactions. *Combust. Flame* **51,** 55–67.

BELLAN J. & HARSTAD, K. 1987 Analysis of the convective evaporation of nondilute clusters of drops. *Int. J. Heat Mass Transfer* **30,** 125–136.

BELLAN, J. & HARSTAD, K. 1988 Turbulence effects during evaporation of drops in clusters. *Int. J. Heat Mass Transfer* **31,** 1655–1668.

CHIANG, C. H. & SIRIGNANO, W. A. 1993 Interacting, convecting, vaporizing fuel droplets with variable properties. *Int. J. Heat Mass Transfer* **36,** 875–886.

CHIANG, C. H., RAJU, M. S. & SIRIGNANO, W. A. 1992 Numerical analysis of convecting, vaporizing fuel droplet with variable properties. *Int. J. Heat Mass Transfer* **35,** 1307–1324.

CONWAY, J. H. & SLOANE, N. J. A. 1988 *Sphere Packings, Lattices and Groups. Series of Comprehensive Studies in Mathematics*, No. 290. Springer-Verlag, New York.

CORREA, S. M. 1981 Group behavior of liquid fuel sprays. Ph.D. Thesis, Univ. of Michigan, Ann Arbor, MI.

DUKOWICZ, J. K. 1980 A particle–fluid numerical model for liquid sprays. *J. Comput. Phys.* **35,** 229–253.

GLENDINNING, A. B. & RUSSEL, W. B. 1982 A pairwise additive description of sedimentation and diffusion in concentrated suspensions of hard spheres. *J. Colloid Interface Sci.* **89,** 124–143.

KIM, I., ELGHOBASHI, S. & SIRIGNANO, W. A. 1992 Three-dimensional flow computation for two interacting, moving droplets. AIAA Paper 92-0343.

KIM, I., ELGHOBASHI, S. & SIRIGNANO, W. A. 1993 Three-dimensional flow over two spheres in parallel side-by-side motion. *J. Fluid Mech.* **246,** 465–488. Also, see AIAA Paper 91-0073.

LABOWSKY, M. & ROSNER, D. E. 1978 "Group" combustion of droplets in fuel clouds. I. Quasi-steady predictions. In *Evaporation–Combustion of Fuel. Advances in Chemistry Series* (Edited by ZUNG, J. T.), No. 166, pp 63–79. American Chemical Society, Washington, DC.

O'ROURKE, P. J. 1989 Statistical properties and numerical implementation of a model for droplet dispersion in a turbulent gas. *J. Comput. Phys.* **83,** 345–360.

ROWE, P. N. & HENWOOD, G. A. 1961 Drag forces in a hydraulic model of a fluidised bed—Part I. *Trans. Instn Chem. Engrs* **39,** 43–54.

SIRIGNANO, W. A. 1983 Fuel droplet vaporization and spray combustion theory. *Prog. Energy Combust. Sci.* **9,** 291–322.

TAL(THAU), R. & SIRIGNANO, W. A. 1981 Heat transfer in sphere assemblages at intermediate Reynolds numbers: a cylindrical cell model. Paper presented at the *ASME Winter A. Mtg*, Washington, DC, ASME Paper 81-WA/HT44.